Nonlinear Operators for Error Diffusion

Tiina Jarske
Nokia Research Center
P.O. Box 100
FIN-33721 Tampere, Finland
E-mail: tiina.jarske @ research.nokia.com

Jaakko T. Astola
Tampere University of Technology
Signal Processing Laboratory
P.O. Box 553 FIN-33101 Tampere, Finland

Abstract

The error diffusion halftoning method preserves details well, but produces some unwanted regular texture patterns. The purpose of this paper is to introduce certain nonlinear operators with small kernels for the error diffusion to reduce the regular patterns. The goal is to suppress pattern artifacts while maintaining a small neighborhood. The method employed uses nonlinear diffusion operators, which possess a relatively complex distribution mechanism, thereby suppressing noticeable patterns. Two nonlinear filter classes are considered: polynomial and median type filters. We found that reduction of regular patterns without producing excessively grainy images is obtained using a combination of linear and median error feedback operators.

1 Introduction

Digital halftoning is needed when displaying continuous-tone images on binary devices (such as displays, laser printers, and fax machines). When the halftoned image consisting of black and white dots is viewed, the image passes through the complex human visual system, which has low pass type characteristics, with the overall effect being that the image appears to have continuous form. The most popular digital halftoning algorithms include ordered dither[1] and error diffusion.[1–4] Recently, more complicated halftoning methods based on the minimization of error metrics (using simulated annealing, neural networks, linear programming, etc.) have been presented.[5–7]

When comparing halftoning algorithms, low- and high-frequency rendition, processing artifacts, and processing complexity are considered. It is well known that the human visual system is less sensitive to errors in high-frequency components than errors in low frequencies. Dithering algorithms are designed to move the halftoning error to the higher frequency components. Ordered dither consists of thresholding the samples of the continuous tone image with a periodic screen (dither matrix) to decide whether to produce a black or white dot. Dither methods can suffer from contour artifacts (though, not as much as simple thresholding methods) and noise-like appearance. Also, the error minimization techniques mentioned above are computationally very demanding. If computation time, imaging process, and hardware of the application allow, an error diffusion method is a good choice, as it can produce higher quality images than ordered dither.

Error diffusion (with a small operator kernel) preserves details well, but produces some unwanted regular texture patterns. The purpose of this paper is to introduce certain nonlinear operators with small kernels for the error diffusion that reduce the regular patterns in the output image. Nonlinear operators generate a more complicated behavior of the error feedback. The use of polynomial and also very nonlinear median type feedback operators can, in theory, lead to more chaotic patterns thus reducing annoying regularities. More complicated halftoning methods that produce aperiodic patterns have been studied by others, e.g., in Ref. 8. We consider two classes of nonlinear filters for the error feedback operator: polynomial (quadratic) and median type filters.

The principles of nonlinear filters are described in Sections 3 and 4. In Section 5, the actual error diffusion operators that are based on the quadratic and median filters are described and the test results are presented. Section 2 gives a brief overview of error diffusion.

2 Error Diffusion

Error diffusion (ED) for binary displays was introduced by Floyd and Steinberg in 1975.[2] In error diffusion (Fig. 1), the image sample (pixel) is compared to a threshold (usually the middle value of the gray scale). If the gray value of the pixel is less than the threshold, it is set to black. Otherwise, the pixel is white. The resulting image consists of black and white dots. The density of the dots determine the gray level. The halftoned binary pixel is compared to the value of the current pixel before thresholding (to which part of the weighted previous er-

ror has been added) and the error is distributed onto unprocessed pixels according to the weights of the error feedback operator. The error feedback operator determines to which pixels the halftoning error is diffused and how much weight is put to these pixels. This is equivalent to filtering the past halftoning errors and adding the filtered error to the present pixel.

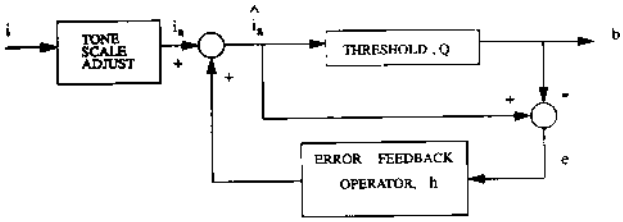

Figure 1. Block diagram of the error diffusion method.

The error diffusion algorithm can be described by the following equations

$$\hat{i}_a(m,n) = i_a(m,n) + \sum_{r,s} h(r,s)e(m-r,n-s), \qquad (1)$$

where $i_a(m,n)$ is the corrected gray level of the original value $i(m,n)$, $h(r,s)$ are the weights of the error diffusion operator, m is the index number of the rows, and n is the index number of the columns. If the gray scale of the input image is $0 \le i(m,n) \le 1$, the threshold operation is described by

$$b(m,n) = Q\left[\hat{i}_a(m,n)\right] = \begin{cases} i, & \text{if } \hat{i}_a(m,n) \ge 1/2 \\ 0, & \text{otherwise,} \end{cases} \qquad (2)$$

where $b(m,n)$ is the quantized (binary) output image and $\hat{i}_a(m,n)$ is the modified (and tone scale corrected) input image. The quantization error that is distributed to the future pixels is

$$e(m,n) = \hat{i}_a(m,n) - b(m,n). \qquad (3)$$

Floyd and Steinberg found that at least four weights (Fig. 2) were needed in order to achieve good results.[2] The Floyd and Steinberg algorithm reproduces fine details well, but some artifacts can be seen: regular patterns and diagonal line structures. Several authors have suggested larger operator masks. Two of those masks are shown in Fig. 2.[4] The operator weights need to be normalized in order to retain the intensity level of the input image. The large operator masks remove the regular patterns that appear when using the Floyd and Steinberg mask (Fig. 7). The algorithm by Jarvis *et al.* is reported to produce sharp edges, e.g., in Ref. 9, but images are grainier than images obtained with the Floyd and Steinberg algorithm. Assuming that the quantization error can be expressed as an uncorrelated noise source $Q(\omega_1,\omega_2)$, the halftoning process is expressed in the frequency domain as

$$B(\omega_1,\omega_2) = I(\omega_1,\omega_2) + [1 - H(\omega_1,\omega_2)]Q(\omega_1,\omega_2), \qquad (4)$$

where $B(\omega_1,\omega_2)$ and $I(\omega_1,\omega_2)$ are the Fourier transforms of the halftoned image and the original image, respectively, and $H(\omega_1,\omega_2)$ is the frequency response of the error filter. For the model of uncorrelated quantization noise, the exact form of the filter and its size do not have an effect on the underlying image. The image and the quantization noise are, of course, highly correlated, meaning that the image will also be subject to filtering. As a result, in practice the filter size has a marked effect on the appearance of halftoned images.[9] For instance, an edge preserving error feed-back operator with large mask size appears to create sharp edges by an "overshooting" type of behavior, as is evident, e.g., in the experiments reported in Ref 10. It would thus be desirable to develop error feedback operators with a small mask that would produce less regular patterns than the Floyd and Steinberg algorithm.

Floyd and Steinberg (1975):

$$\begin{array}{ccc} & \bullet & 7 \\ 3 & 5 & 1 \end{array}$$

Jarvis, Judice, and Ninke (1976):

$$\begin{array}{ccccc} & & \bullet & 7 & 5 \\ 3 & 5 & 7 & 5 & 3 \\ 1 & 3 & 5 & 3 & 1 \end{array}$$

Stucki (1981):

$$\begin{array}{ccccc} & & \bullet & 8 & 4 \\ 2 & 4 & 8 & 4 & 2 \\ 1 & 2 & 4 & 2 & 1 \end{array}$$

Figure 2. Operator masks for the error diffusion.

Comparison of error diffusion algorithms is complicated, because the visual quality of the resulting image depends also on the tone scale of the original image. In practice, for a given device and halftoning method, one can optimize the visual quality of halftones by adjusting the tone scale of the original image.[4] If contrast enhancement is desired, the midrange gray levels can be mapped to lighter values and the number of gray levels can be reduced so that several light gray values are mapped to 255 (the maximum gray value) and several dark gray values to 0. Figure 3[4] shows an example of this kind of mapping.

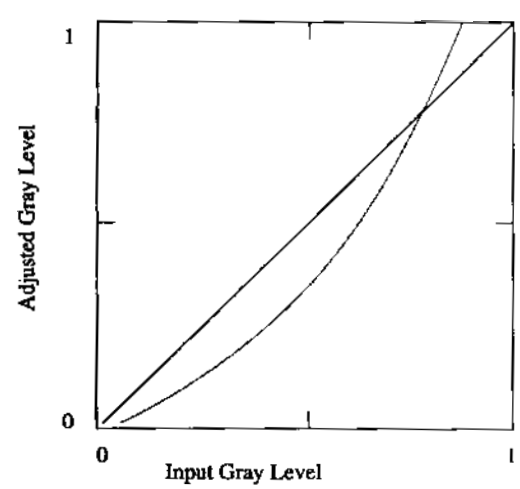

Figure 3. An example of tone scale adjustment. The straight line is a reference for no-change transformation.

3 Quadratic Operators

If an error diffusion operator has a large mask size, its behavior on different types of edges becomes difficult to control. Thus, we wish to keep the mask size as small as possible. Furthermore, the use of a small operator mask simplifies the implementation. To keep the mask size small (four coefficients) and to reduce the regular patterns of the halftoned image, one possibility is to use a nonlinear error diffusion operator. The goal would be to obtain behavior that would be chaotic in the sense that no annoying periodicities would be produced. An interesting nonlinear filter class is the class of polynomial (or Volterra) filters.[11–13] The input-output relation of the polynomial filter is expressed in the form of a truncated discrete Volterra series. The second-order Volterra filter consisting of a parallel combination of linear and quadratic filters has been successfully used to improve the performance of linear filters.[11–13] These filters are called quadratic filters. It is well known that increasing the degree of a polynomial system will, in general, lead to systems with more complicated behavior. In the case of error diffusion, our experiments indicate that quadratic operators have high enough order to obtain sufficient nonlinearity to reduce the regularities in the halftoned images. Higher order terms do not have much effect on the results.

A useful property of polynomial filters is that the output depends linearly on the filter coefficients. This characteristic is important in the analysis and design of polynomial filters. Polynomial filters are described by the discrete Volterra series (for the 1–D case) as follows:

$$y(n) = h_0 + \sum_{k=1}^{\infty} \bar{h}_{k1}[x(n)], \tag{5}$$

where

$$\bar{h}_{k1}[x(n)] = \sum_{i_{11}=0}^{\infty} \cdots \sum_{i_{k1}=0}^{\infty} h_{k1}(i_{11},\ldots i_{k1}) \cdot x(n-1_{11})\ldots x(n-i_{k1}). \tag{6}$$

In the above formulas, h_0 is a constant (offset) term, $h_1(i_1)$ is the impulse response of a linear IIR filter, and $h_k(i_1,...,i_k)$ can be considered as a generalized k'th-order impulse response (i.e., the nonlinear part of the filter). A complete quadratic filter is then described by the first three terms of the Volterra series. For the 2-D case the linear operator (k = 1) can be expressed by

$$\bar{h}_{12}[x(n_1,n_2)] = \sum_{i_{11}=0}^{N_1-1} \sum_{i_{12}=0}^{N_2-1} h_{12}(i_{11},i_{12}) \cdot x(n_1-i_{11},n_2-i_{12}), \tag{7}$$

where N_1, N_2 is the size of the filter kernel. The nonlinear (quadratic) operator for the 2-D case is expressed by

$$\bar{h}_{22}[x(n_1,n_2)] = \sum_{i_{11}=0}^{N_1-1} \sum_{i_{12}=0}^{N_2-1} \sum_{i_{21}=0}^{N_1-1} \sum_{i_{22}=0}^{N_2-1} h_{22}(i_{11},i_{12},i_{21},i_{22}) \cdot x(n_1-i_{11},n_2-i_{12}), \cdot x(n_1-i_{21},n_2-i_{22}). \tag{8}$$

In general, to preserve any constant input gray level the constant term of the quadratic filter should be zero, the sum of the linear filter coefficients should be one, and the sum of the coefficients of quadratic terms zero.[13] However, in the case of error diffusion (with a linear operator), all the operator coefficients should be positive and sum to one.[4] The quadratic error diffusion operator structures that we tested are shown in Sec. 5.

4 Median Type Operators

In addition to the quadratic operators, we studied the use of median type operators in reducing the regular patterns produced by error diffusion. The median filter and median type filters are widely used in image processing applications as they remove impulsive noise while retaining edges. Because the median operation is based on ordering relation, it is highly nonlinear. Thus, it is not possible to have a polynomial filter of low order exhibiting similar performance. This indicates that median type filters could be useful in the feedback loop. The median filter for digital signal processing was first presented by Tukey in 1974, cf. in Ref. 14. It is defined by

$$Y(n) = \mathrm{MED}[X(n-K),...,X(n),...,X(n+K), \tag{9}$$

where $X(n)$ and $Y(n)$ are the input and output signals, respectively. The filter length is $N = 2K + 1$. The median is the centermost sample value of the ordered input sequence:

$$\begin{aligned} &\text{if} && X_{(1)} \le X_{(2)} \le \ldots \le X_{(2K+1)} \\ &\text{then} && \mathrm{MED}[X_1,X_2,...,X_{2K+1}] = X_{(K+1)} \end{aligned} \tag{10}$$

As can be seen, the output of the median filter is one of the input sample values.

The median filter has been generalized to allow the weighting of the samples by Justusson, cf. in Ref. 15. Non-negative weights are assigned to all the samples inside the filter window. The weights denote the number of repetitions for each input sample inside the filter window. For an ordered input sequence the weighted median (WM) filter can be compactly expressed by

$$Y(n) = \mathrm{MED}[W_{-L} \lozenge X(n-L),..., W_0 \lozenge X(n),..., W_R \lozenge X(n+R)], \tag{11}$$

where $W_{-L},..., W_0,...,W_R$ are the weights, $W \lozenge X$ means repeating the sample X W times, and L, R denote the left-most and the right-most samples, respectively. The weighted median filters have been shown to belong to the class of stack filters.[16,17]

5 Experimental Results

5.1 Quadratic Error Diffusion Operators

We tested several types of quadratic error diffusion operators. The optimal weights for both the linear part and the quadratic part of the quadratic ED operator were determined experimentally. We used the same mask as in the linear error diffusion case:

$$\boxed{\begin{matrix} e_{m-1,n-1} & e_{m-1,n}\, e_{m-1,n+1} \\ e_{m,n-1} & X_{m,n} \end{matrix}}, \quad \boxed{\begin{matrix} \delta\gamma\beta \\ \alpha \end{matrix}} \tag{12}$$

where $e_{m,n-1}$, $e_{m-1,n+1}$, $e_{m-1,n}$, and $e_{m-1,n-1}$ are the quantization errors for the corresponding input pixels. The pixel X is the current pixel to be halftoned. The constant term h_0 [Eq. (5)] is set to zero. Let us use the following shorthand notation for the indices $\alpha = (m,n-1)$, $\beta = (m-1,n+1)$, $\gamma = (m-1,n)$, and $\delta = (m-1,n-1)$. For example, $e_{m,n-1}e_{m-1,n+1} = e_\alpha e_\beta$. As a result, the linear part of the quadratic filter [Eq. (7)] is described by

$$f_{\mathrm{LIN}} = a_\alpha e_\alpha + a_\beta e_\beta + a_\gamma e_\gamma + a_\delta e_\delta, \tag{13}$$

where a_i's are the linear filter coefficients:

$$\boxed{\begin{matrix} & X_{m,n} & a_\alpha \\ a_\beta & a_\gamma & a_\delta \end{matrix}}. \tag{14}$$

The nonlinear part of the quadratic filter for the above pixels is obtained from Eq. (8):

$$\begin{aligned} f_{\mathrm{QUAD}} = {} & c_{\alpha,\alpha}e_\alpha^2 + c_{\alpha,\beta}e_\alpha e_\beta + c_{\alpha,\gamma}e_\alpha e_\gamma + c_{\alpha,\delta}e_\alpha e_\delta \\ & + c_{\beta,\alpha}e_\beta e_\alpha + c_{\beta,\beta}e_\beta^2 + c_{\beta,\gamma}e_\beta e_\gamma + c_{\beta,\delta}e_\beta e_\delta \\ & + c_{\gamma,\alpha}e_\gamma e_\alpha + c_{\gamma,\beta}e_\gamma e_\beta + c_{\gamma,\gamma}e_\gamma^2 + c_{\gamma,\delta}e_\gamma e_\delta \\ & + c_{\delta,\alpha}e_\delta e_\alpha + c_{\delta,\beta}e_\delta e_\beta + c_{\delta,\gamma}e_\delta e_\gamma + c_{\delta,\delta}e_\delta^2, \end{aligned} \tag{15}$$

where the quadratic coefficients can be expressed as the matrix

$$\mathbf{C} = \begin{bmatrix} c_{\alpha,\alpha} & c_{\alpha,\beta} & c_{\alpha,\gamma} & c_{\alpha,\delta} \\ c_{\beta,\alpha} & c_{\beta,\beta} & c_{\beta,\gamma} & c_{\beta,\delta} \\ c_{\gamma,\alpha} & c_{\gamma,\beta} & c_{\gamma,\gamma} & c_{\gamma,\delta} \\ c_{\delta,\alpha} & c_{\delta,\beta} & c_{\delta,\gamma} & c_{\delta,\delta} \end{bmatrix}. \tag{16}$$

Obviously, we can choose the matrix $\mathbf{C}$ to be symmetric, i.e, $c_{\zeta,\eta} = c_{\eta,\zeta}$, $\zeta,\eta \in \{\alpha,\beta,\gamma,\delta\}$.

We tested the quadratic error diffusion operator for different kinds of images, a slowly varying gray wedge and natural images. Figure 4 shows the gray wedge test image. For the natural test images, we applied the tone scale adjustment,[4] to yield halftoned images with increased contrast. As image quality metrics are difficult to apply in the present settings, the performance of the different methods was evaluated visually.

It was found that the requirement of the sum of the quadratic coefficients to be zero (Sec. 5) results in low-quality halftoned images and thus only positive coefficients were used. Also, the sum of all error diffusion coefficients was set equal to one in order to keep the quantization error bounded.

The results for a quadratic ED operator with $a_{1,0}$ = 14/46, $a_{-1,1}$ = 8/46, $a_{0,1}$ = 12/46, $a_{1,1}$ = 6/46, and c_i = 1/46,

$$\begin{aligned} a_i &= [a_\alpha, a_\beta, a_\gamma, a_\delta] = (1/46)\times[14,8,12,6], \\ c_i &= (1/46)\times\begin{bmatrix} 1 & 1 & 1 & 1 \\ 1 & 1 & 1 & 1 \\ 1 & 1 & 1 & 1 \\ 1 & 1 & 1 & 1 \end{bmatrix}, \end{aligned} \tag{17}$$

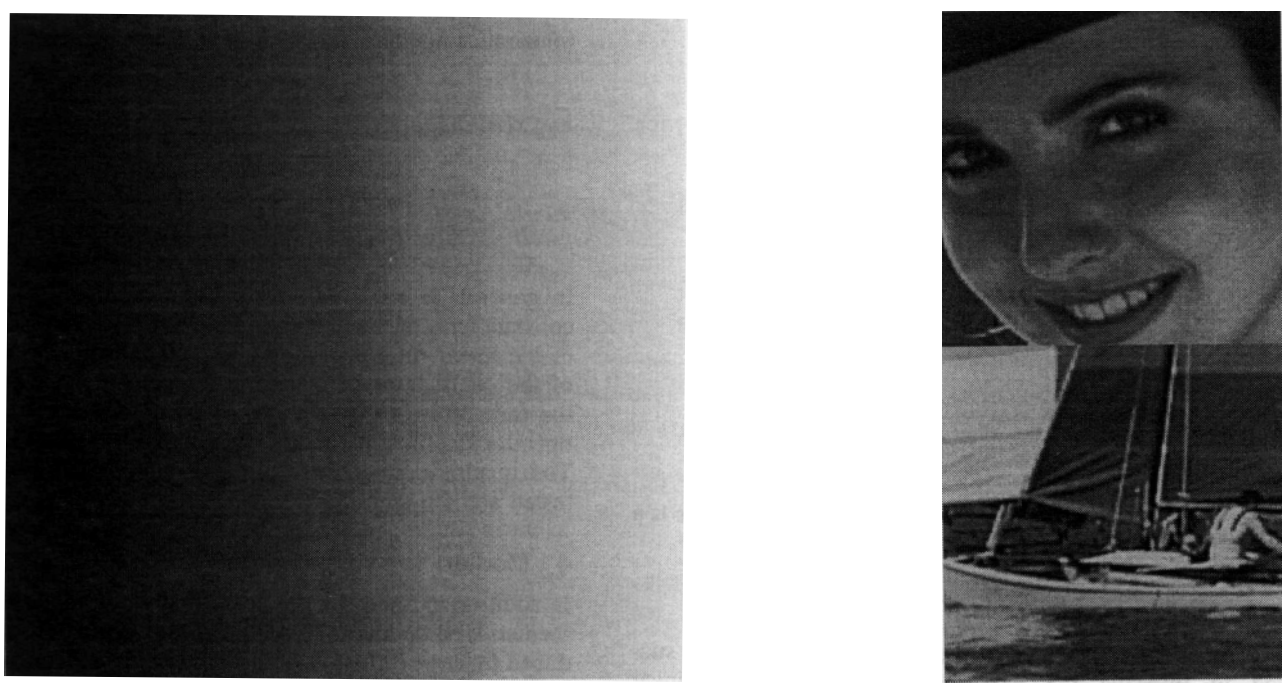

Figure 4. The original test images: (a) gray wedge, (b) girl, and (c) yachts.

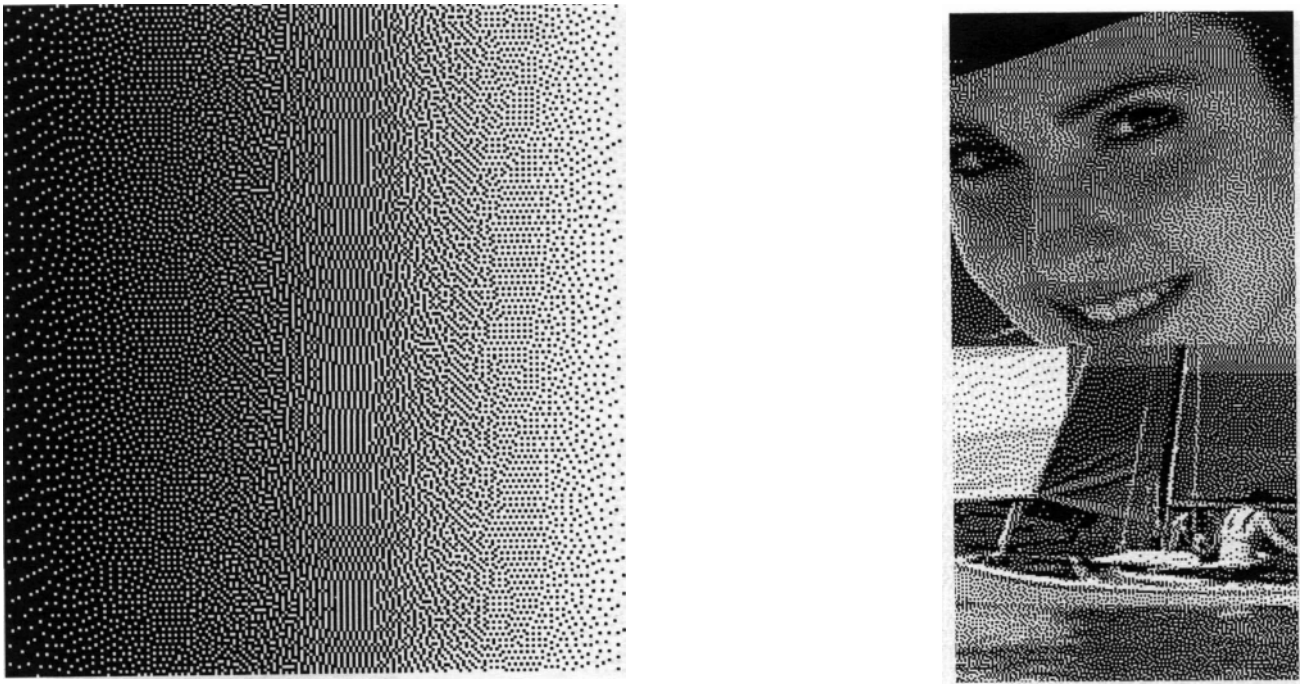

Figure 5. Halftoned images using the quadratic error diffusion operator (with all the quadratic coefficients).

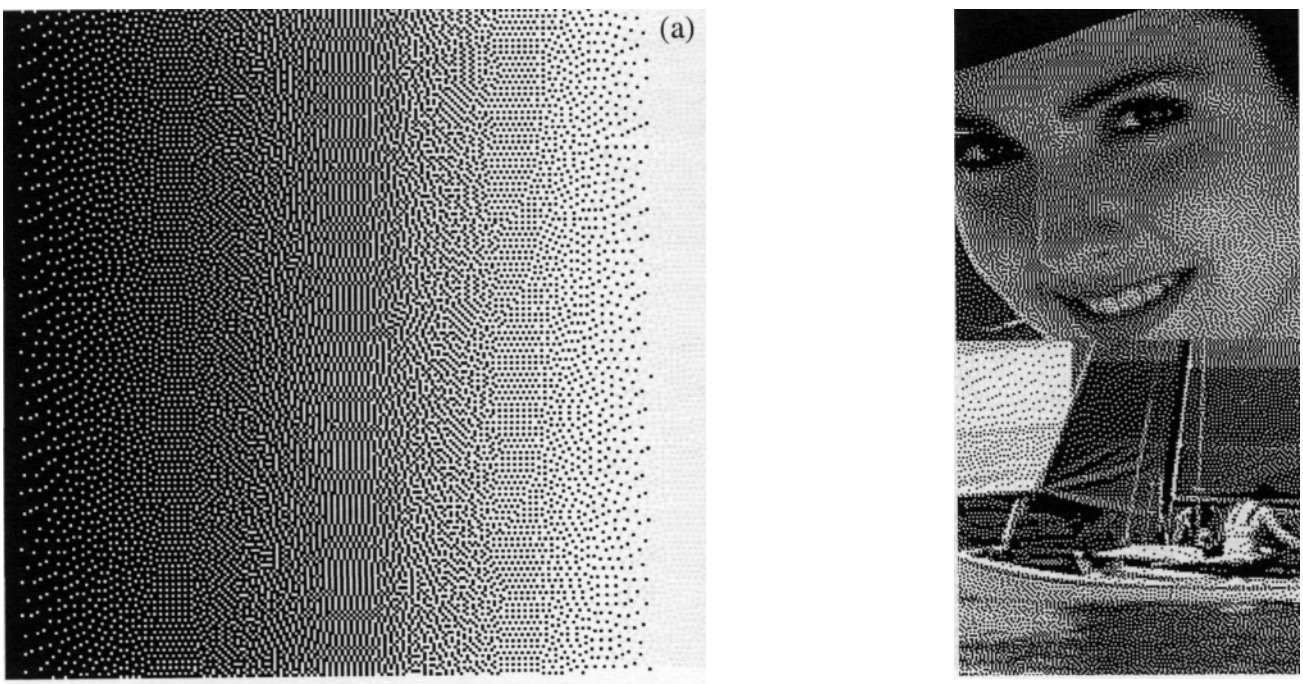

Figure 6. Halftoned images using the quadratic error diffusion operator (with the diagonal quadratic coefficients).

are shown in Fig. 5. The above mentioned linear coefficients, a_i, were found to be the best. The results indicate that all the practical advantage of the quadratic terms can be achieved by using only the diagonal quadratic coefficients. The following weights

$$a_i = [a_\alpha, a_\beta, a_\gamma, a_\delta] = (1/47) \times [14, 8, 12, 6],$$

$$c_i = (1/47) \times \begin{bmatrix} 3 & 0 & 0 & 0 \\ 0 & 1 & 0 & 0 \\ 0 & 0 & 2 & 0 \\ 0 & 0 & 0 & 1 \end{bmatrix} \tag{18}$$

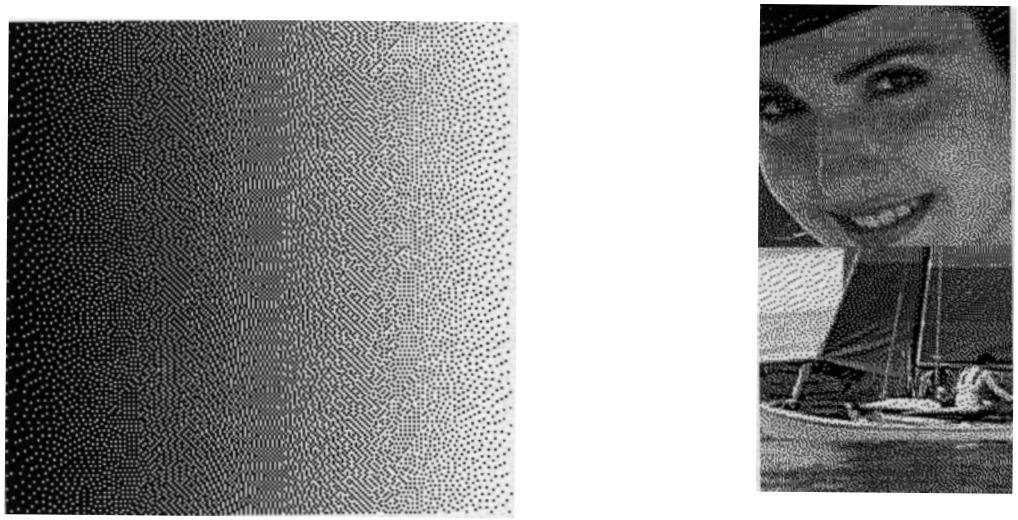

(a)

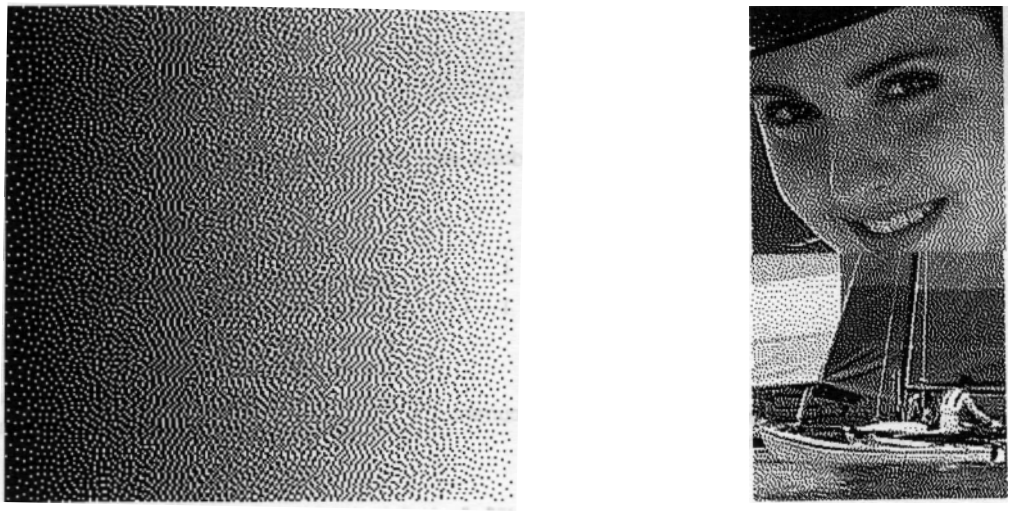

(b)

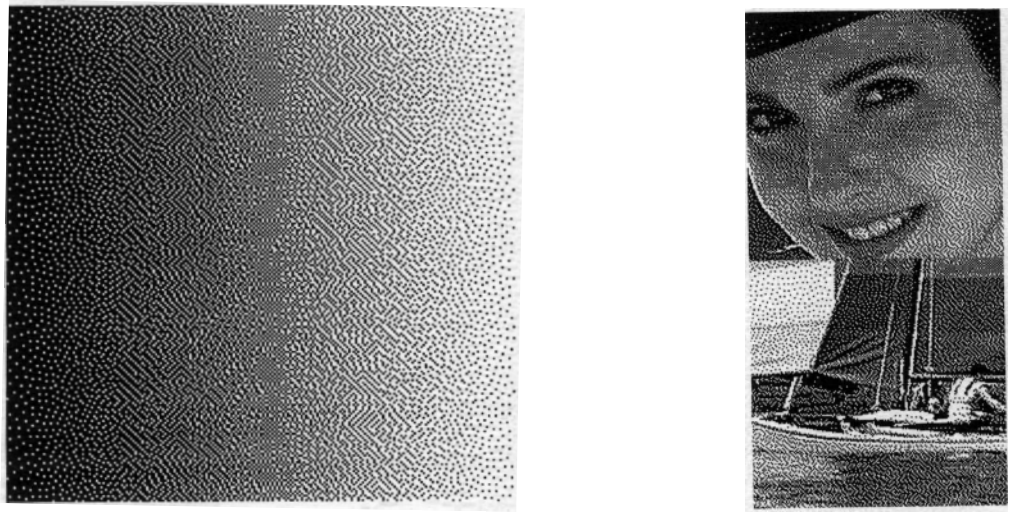

(c)

Figure 7. Halftoned images using linear error diffusion operators: (a) Floyd and Steinberg operator, (b) Jarvis, Judice, and Ninke operator, and (c) Stucki operator.

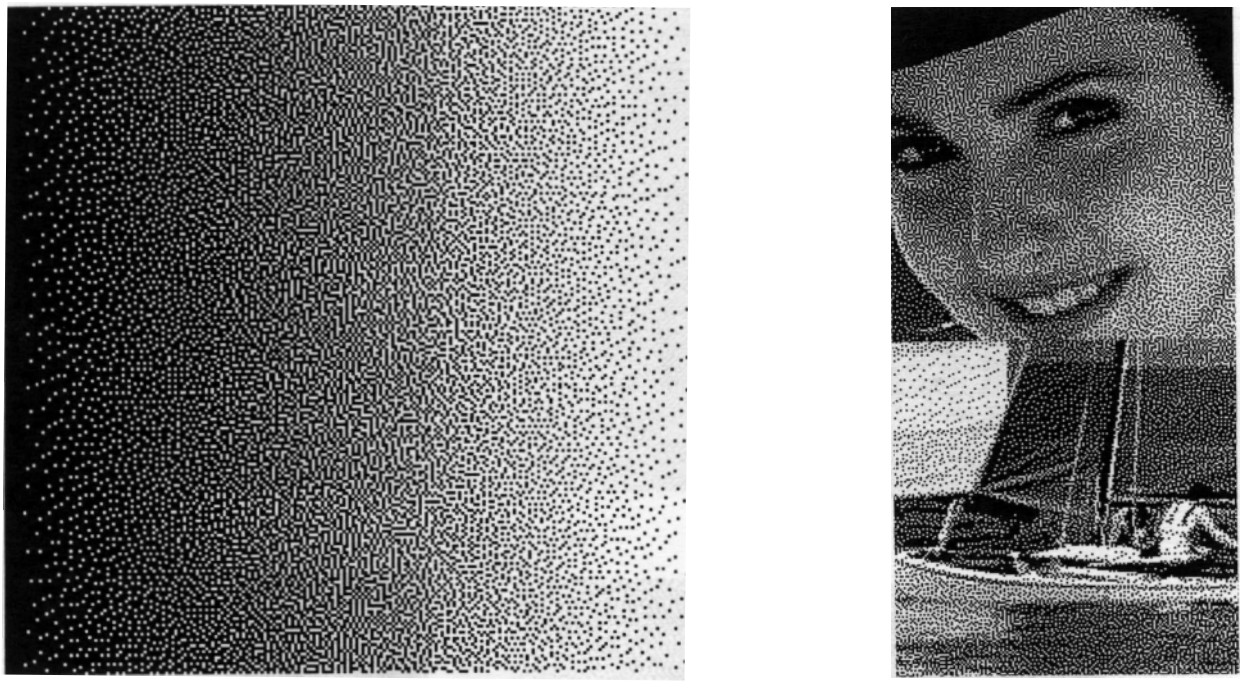

Figure 8. Halftoned images using the quadratic error diffusion operator (a)Fig. 6 with a 30% random threshold.

give fairly good results. The images have a clear appearance, partly resulting from fewer gray levels (Fig. 6). Comparing these images to the linear (Floyd and Steinberg, $a_{1,0} = 7/16$, $a_{-1,1} = 3/16$, $a_{0,1} = 5/16$, $a_{1,1} = 1/16$, Fig. 2) ED filter, Fig. 7(a), shows that the regular patterns are considerably reduced. Figures 7(b) and 7(c) show the results for the bigger error diffusion masks of Fig. 2. These images lack disturbing regular patterns, but they are more grainy than the images obtained with a smaller mask.

The regular patterns of the error diffused images can be further reduced by perturbing the operator coefficients or the threshold. We tested the effect of perturbing the threshold both for the linear and nonlinear ED operators. Figure 8 shows the results for the quadratic ED operator of Fig. 6 with a perturbated threshold. The threshold was randomly selected between the limits obtained by adding to and subtracting from the threshold 30% of the fixed value. It can be seen that the regular patterns have totally disappeared, but the images have grainy appearance.

5.2 Median Type ED Operators

We expected that the good properties of the median would also show in this application. We used the weighted median (WM) error diffusion operator [Fig. 9(a)] described by

$$\mathrm{MED9}[3 \lozenge e_{m,n-1}, 2 \lozenge e_{m-1,n+1}, 3 \lozenge e_{m-1,n}, e_{m-1,n-1}]. \quad (19)$$

The WM ED operator performs the halftoning operation correctly, but as can be seen from Fig. 10, the halftoned values change too slowly. Changing the weights does not improve the performance of the WM ED operator. We also tested larger filter masks [Figs. 9(b) and 9(c)], but the resulting images were more coarse than with the smaller mask.

$$\begin{array}{ccc} 1 & 3 & 2 \\ 3 & \bullet & \end{array} \qquad \begin{array}{cccc} & 1 & 1 & 1 \\ & 1 & 1 & 1 & 1 \\ 1 & 1 & \bullet & \end{array} \qquad \begin{array}{cccc} & 1 & 1 & 1 \\ & 1 & 2 & 1 & 1 \\ 1 & 2 & \bullet & \end{array}$$

(a) (b) (c)

Figure 9. Masks for the WM error diffusion operator. ● is the current pixel to be halftoned. The numbers denote the weights.

As the WM error diffusion operator does not work very well alone, we combined it with the polynomial ED operator:

$$\mathrm{MED9}[2 \lozenge e_{m,n-1}, e_{m-1,n+1}, 2 \lozenge e_{m-1,n}, e_{m-1,n-1}, 2 \lozenge e_{m,n-1}e_{m-1,n}, e_{m-1,n+1}e_{m-1,n-1}]. \quad (20)$$

The results were not good, as $e_{m,n-1}e_{m-1,n}$ and $e_{m-1,n+1}e_{m-1,n-1}$ change the signal level, i.e., give darker images than the original ones. When dividing $e_{m,n-1}e_{m-1,n}$ and $e_{m-1,n+1}e_{m-1,n-1}$ by one of the error values and changing the weights somewhat,

$$\mathrm{MED9}[3 \lozenge e_{m,n-1}, 2 \lozenge e_{m-1,n+1}, 2 \lozenge e_{m-1,n}, e_{m,n-1} \times e_{m-1,n}/(e_{m-1,n+1}+1), e_{m-1,n+1}e_{m-1,n-1}/(e_{m,n-1}+1)], \quad (21)$$

we obtained better results (Fig. 11). However, disturbing line structures are clearly seen. The reason for the poor behavior of the WM filter in error diffusion is prob-

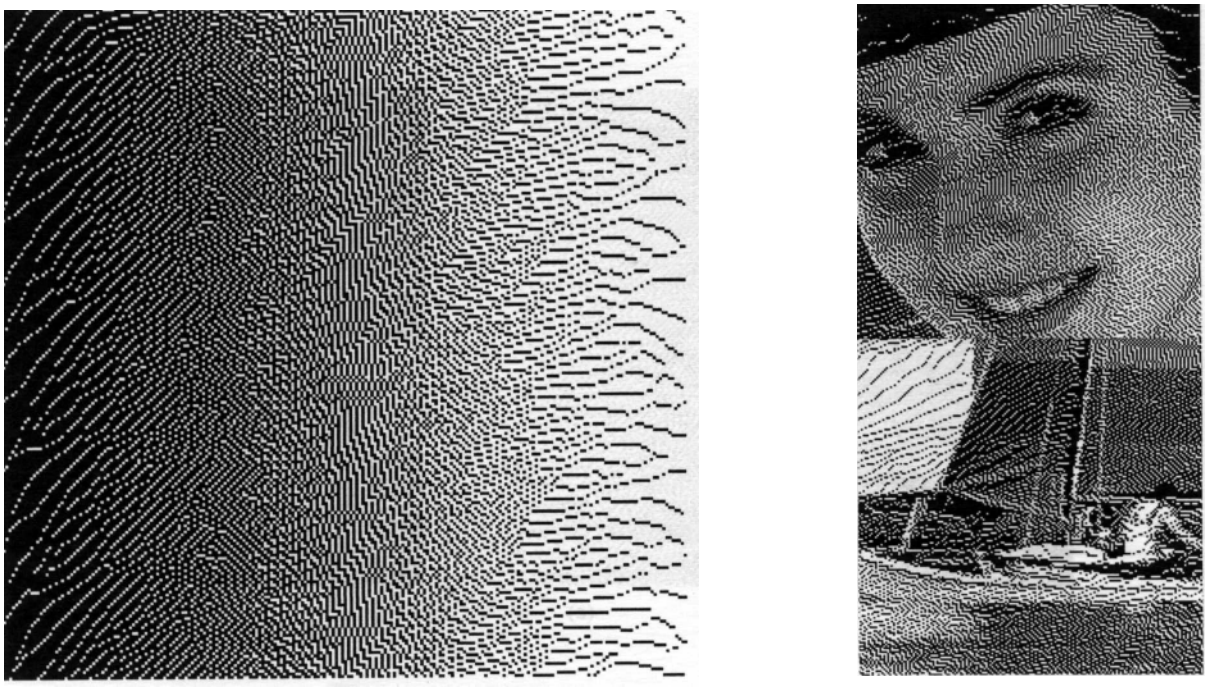

Figure 10. Halftoned images using the weighted median error diffusion operator [Fig. 9(a)].

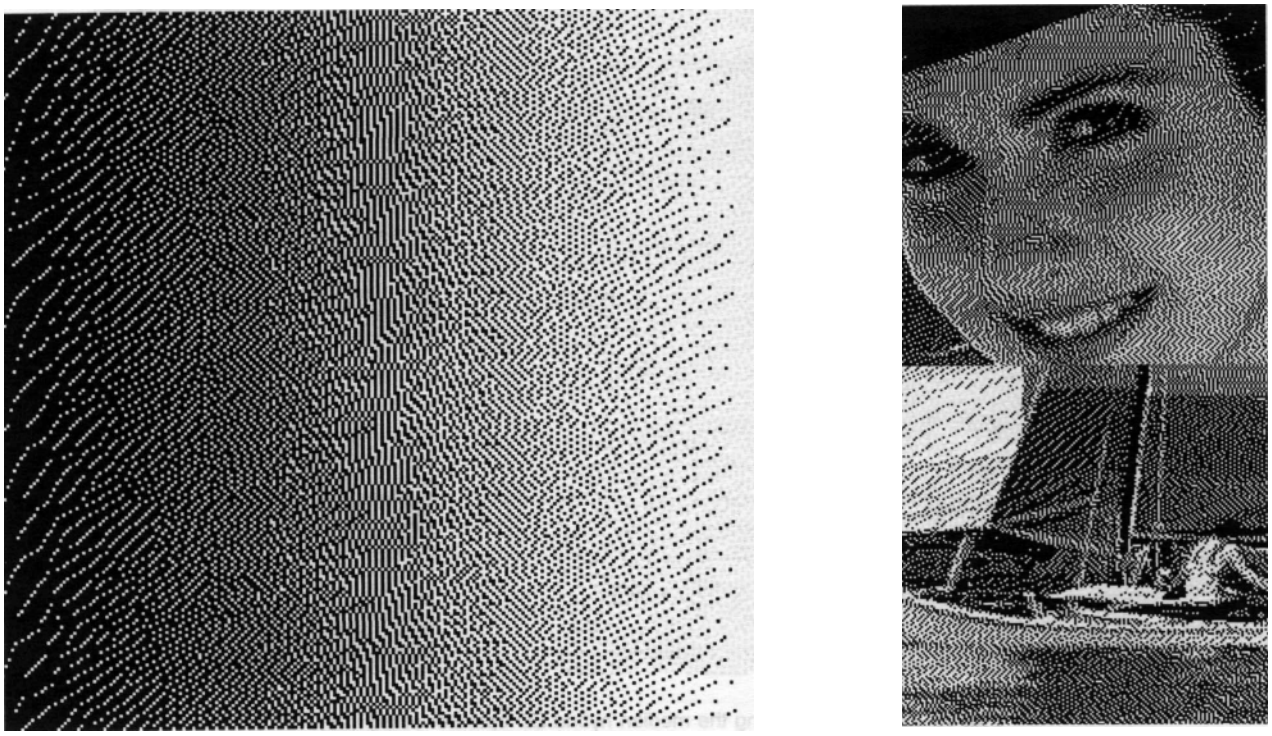

Figure 11. Halftned images using the combined weighted median and polynomial error diffusion operator.

ably that its operation is somewhat too coarse and therefore small differences cannot be distinguished.

A median hybrid ED operator offers an interesting possibility, as it combines linear operations with the nonlinear median operation. Detail preservation is achieved through the small subfilters, and the median operation reduces the regular patterns. We tested different combinations of linear subfilters with mask sizes four and five. The filter mask and the median hybrid ED filter for mask size four are

$$\boxed{\begin{matrix} e_{m-1,n-1} & e_{m-1,n} & e_{m-1,n+1} \\ e_{m,n-1} & X_{m,n} & \end{matrix}} \tag{22}$$

$$\mathrm{MED3}\begin{cases} e_{m,n-1} + e_{m-1,n} - e_{m-1,n-1} \\ e_{m,n-1}/2 + (e_{m-1,n+1} + e_{m-1,n)/4} \\ (2e_{m,n-1} + e_{m-1,n+1} + e_{m-1,n} + e_{m-1,n-1})/5. \end{cases} \tag{23}$$

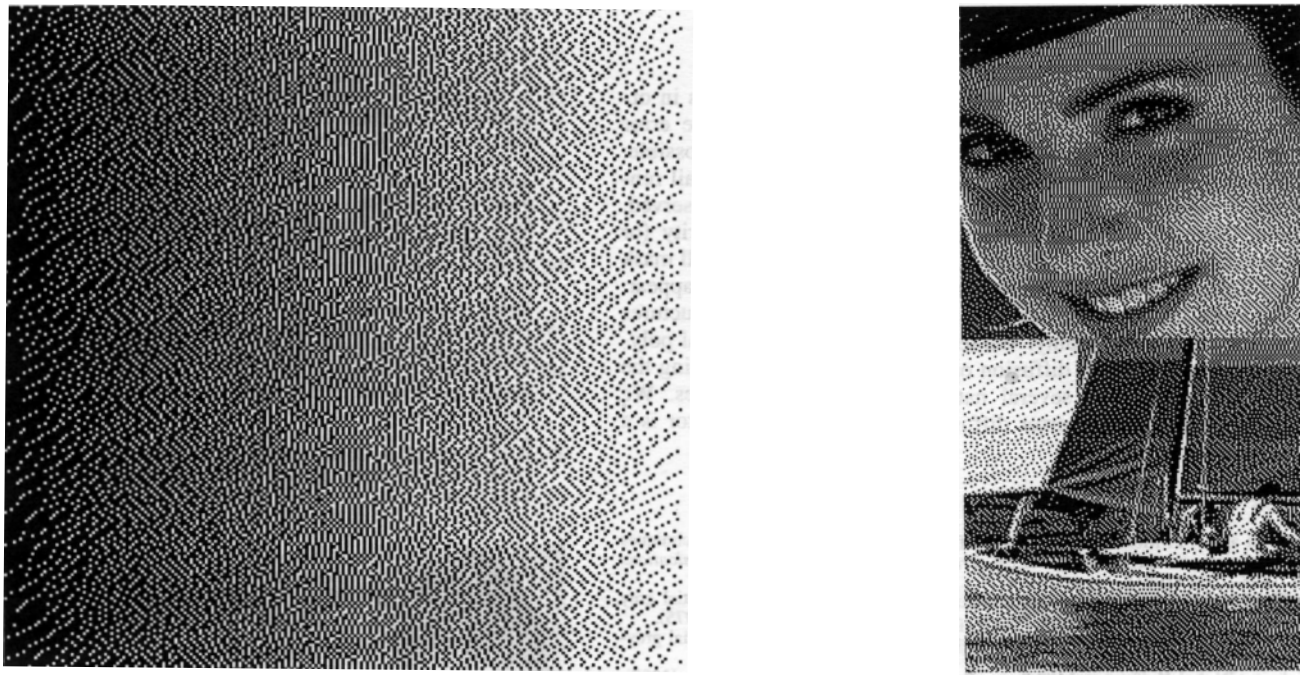

Figure 12. Halftoned images using the mediam hybrid ED operator of Eq. (23).

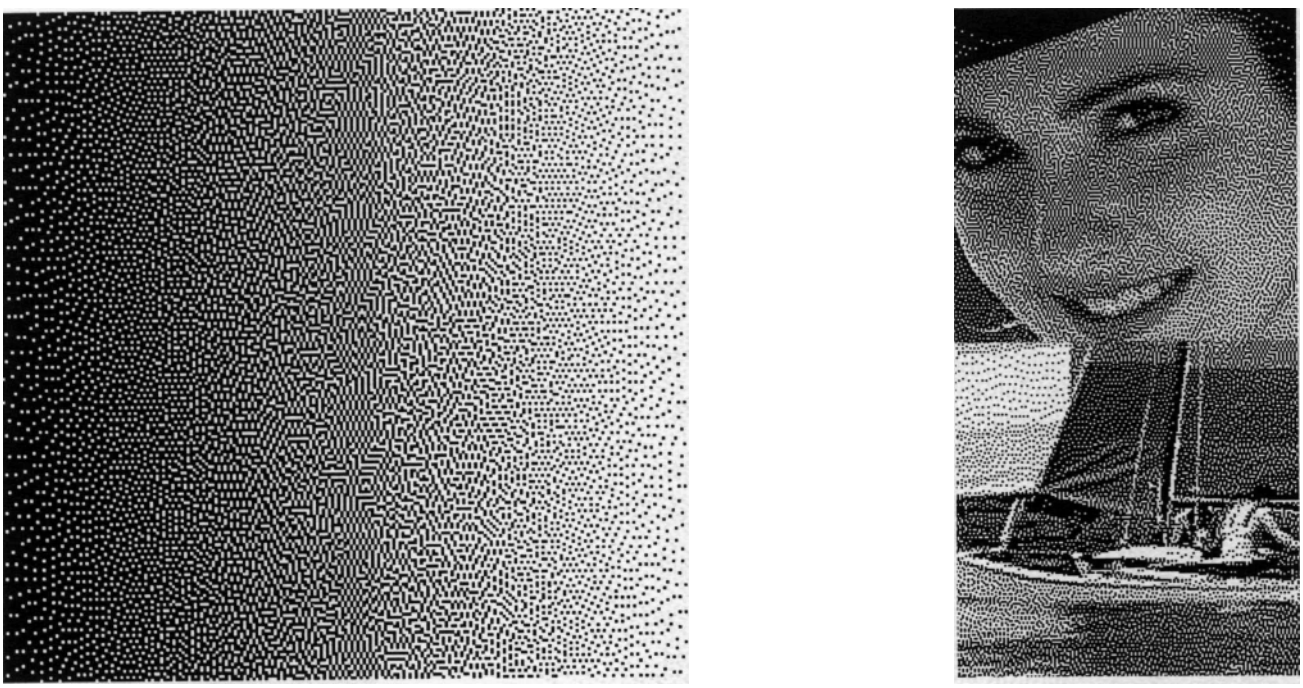

Figure 13. Halftoned using the median hybrid ED operator of Eq. (25).

The result of using the above mentioned median hybrid ED operator for the gray wedge image is shown in Fig. 12. It can be seen from the image that regular patterns are still visible.

We added one more pixel to the mask in order to make the median hybrid ED operator as symmetric as possible. The mask and the corresponding median hybrid operator are

$$\boxed{\begin{matrix} & e_{m-2,n} & \\ e_{m-1,n-1} & e_{m-1,n} & e_{m-1,n+1} \\ e_{m,n-1} & X_{m,n} & \end{matrix}} \tag{24}$$

$$\mathrm{MED3}\begin{cases} (e_{m,n-1}+e_{m-1,n})/2 \\ (e_{m-1,n+1}+e_{m-1,n+1})/2 \\ (e_{m,n-1}+e_{m-1,n+1}+e_{m-1,n} \\ \quad +e_{m-1,n-1}+e_{m-2,n})/5. \end{cases} \tag{25}$$

Figure 13 shows the results after halftoning the test images with the median hybrid ED operator of Eq. (25). It can be seen from the gray wedge image that regular structures are reduced considerably. In addition, the

structure of patterns is finer than using the Jarvis *et al.* operator. Thus, the suggested algorithm preserves better fine details. Especially, the middle gray regions are well rendered. The median operation is simple, as it is taken only over three samples. The subfilters enable the use of the simple median operation.

However, memory requirement is increased due to the additional pixel (compared to the Floyd and Steinberg ED operator).

6 Conclusions

We have introduced nonlinear error diffusion filters in order to reduce the annoying regular patterns of the error diffused halftones using as small a mask size as possible. Besides reducing the regular patterns, the good detail rendition of the error diffusion method should be preserved. Furthermore, there is a trade-off between granularity (or detail preservation) and regular structures. With small mask sizes, fine details are preserved, but regular patterns appear. With large masks, on the other hand, no regular structures are present, but images are grainy. We tested several polynomial and median type error diffusion operators using the gray wedge test image and several natural images. We found that the median hybrid error diffusion operator is a good compromise.

References

1. J. C. Stoffel and J. F. Moreland, "A survey of electronic techniques for pictorial image reproduction," *IEEE Trans. Communications* **29**(12), 1898–1924 (1981).
2. R. W. Floyd and L. Steinberg, "Adaptive algorithm for spatial grey scale," *SID Int. Sym. Digest of Tech. Papers*, pp. 36–37 (1975).
3. R. W. Floyd and L. Steinberg, "Adaptive algorithm for spatial grey scale," *Proc. SID* **17**(2), 75–77 (1976).
4. R. Ulichney, *Digital Halftoning*, MIT Press, Cambridge, MA (1987).
5. J. B. Mulligan and A. J. Ahumada, Jr., "Principled halftoning based on human vision models," *Proc. SPIE, Human Vision, Visual Processing, and Digital Display* **1666**, 109–121 (1992).
6. C. H. Chu and W. Watunyuta, "On designing dither matrices using human visual model," *Proc. SPIE, Human Vision, Visual Processing, and Digital Display* **1666**, 134–143 (1992).
7. A. Zakhor, S. Lin, and F. Eskafi, "A new class of B/W halftoning algorithms," *IEEE Trans. Image Processing*, **2**(4), 499–509 (1993).
8. L. Velho and J. de Miranda Gomes, "Digital halftoning with space filling curves," *Computer Graphics* **25**(4), 81–90 (July 1991).
9. S. Weissbach and F. Wyrowski, "Error diffusion procedure: theory and applications in optical signal processing," *Applied Optics* **31**(14), 2518–2534 (1992).
10. Z. Fan and F. Li, "Edge behavior of error diffusion," in *Proc. IEEE Int. Conf. Image Processing*, Washington DC, pp. 113–116 (1995).
11. T. Koh and E. J. Powers, "Second-order Volterra filtering and its application to nonlinear system identification," *IEEE Trans. Acoustics, Speech, and Signal Processing* **33**(6), 1445–1455 (1985).
12. G. Ramponi and G. L. Sicuranza, "Quadratic digital filters for image processing," *IEEE Trans. Acoustics, Speech, and Signal Processing* **36**(6), 937–939 (1988).
13. G. L. Sicuranza, "Quadratic filters for signal processing," *Proc. IEEE* **80**(8), 1263–1285 (1992).
14. N. C. Gallagher, Jr., and G. L. Wise, "A theoretical analysis of the properties of median filters," *IEEE Trans. Acoustics, Speech, and Signal Processing* **29**(6), 1136–1141 (1981).
15. I. Pitas and A. N. Venetsanopoulos, *Nonlinear Digital Filters, Principles and Applications*, Kluwer Academic Publishers (1990).
16. O. Yli-Harja, J. Astola, and Y. Neuvo, "Analysis of the properties of median and weighted median filters using threshold logic and stack filter representation," *IEEE Trans. Signal Process*. **39**, 395–410 (Feb. 1991).
17. P. D. Wendt, E. J. Coyle, and N. C. Gallagher, Jr., "Stack filters," *IEEE Trans. Acoustics, Speech, and Signal Processing* **34**(4), 898–911(1986).

❋ Previously published in the *Journal of Electronic Imaging*, **6**(3) pp. 357–366, 1997.